EUROPEAN ORGANISATION FOR NUCLEAR RESEARCH

CERN/DRDC/91-54
DRDC/P34
January 13th, 1992

A Silicon Hadron Calorimeter module operated in a strong magnetic field with VLSI read out for LHC

F. Carminati, M. Della Negra, S. Giani, M. Glaser, A. Hervé,
J. M. Le Goff, F. Lemeilleur, M. Pimiä, E. Radermacher** and H. Verweij.
CERN, Geneva, Switzerland

M. Baturitsky[2], V. Chalyshev, A. Cheremukhin, B. Eidelman[3], V. Eremin[4], S. Golubykh,
I. Golutvin*, L. Ivanjutin[1], V. Izhevsky[1], V. Kalagin, V. Kharlamov[3], Y. Kozlov[1],
P. Kuchinsky[2], V. Lomako[2], S. Losanu, I. Lukyanov, S. Makarov[1], I. Merkin,
M. Milvidsky[1], V. Minashkin, D. Peshekhonov,V. Petrov[2], A. Rashevsky, I. Savin,
S. Sergeev, N. Shumeiko[2], A. Sidorov[1], N. Susova, A. Vasilesku, E. Verbitskaya[4],
A. Yaremchuk[3], V. Yavid[2], N. Zamyatin, V. Zhiltsov, V. Zubarev and V. Zverolovlev[3]
Joint Institute for Nuclear Research (JINR), Dubna, RSFSR

A. Baldini, M. Bocciolini, E. Borchi, A. Cartacci, C. Civinini, R. D'Alessandro, E. Gallo,
M. Meschini, M. Pieri and P. Spillantini
Dipartimento di Fisica dell'Università and INFN Sezione di Firenze, Italy

M. Acciarri, P. G. Avanzini[5], A. Baschirotto, S. Benetti, G. Cai[5], R. Castello, C. Furetta,
A. Gola[6], P. Menniti[6], R. Paludetto, S. Pensotti, S. Pizzini, P. G. Rancoita, M. Rattaggi and
G. Terzi
INFN Sezione di Milano, Italy

H. R. Brashear, C. L. Britton, H. O. Cohn and R. Todd
Oak Ridge National Laboratory, Oak Ridge, U. S. A

L. Barone, B. Borgia* , M. Diemoz, E. Longo and G. Organtini
Dipartimento di Fisica dell'Università and INFN Sezione di Roma, Italy

P. Berridge, S. Berridge, W. M. Bugg, Y. C. Du, H. J. Hargis, R. Kroeger, I. Tsveybak
and A. Weidemann
Physics Dept., University of Tennessee, Knoxville, U. S. A

F. Szoncso, G. Walzel and C.- E. Wulz
HEPHY, Österreichische Akademie der Wissenschaften, Vienna, Austria

* Joint Spokesmen
** Contact person
- Collaborators from industry (Ansaldo, ELMA, SGS-THOMSON, SIAPS) are listed under collaborating institutes

[1] Research and Production Association ELMA, Zelenograd, RSFSR
[2] Byelorussian State University, Minsk, Byelorussia.
[3] Research and Production Company SIAPS, Zelenograd, RSFSR.
[4] Joffe Physical-Technical Institute, St. Petersburg, RSFSR
[5] Ansaldo Ricerche spa, Genoa, Italy.
[6] SGS-THOMSON, Castelletto (Milan), Italy.

ABSTRACT

On the basis of a cost optimized technology of Silicon detectors production we propose to build a prototype of LHC hadron calorimeter module. This calorimeter module will include signal routing, mounting boards, complete front-end electronics including tower sums and pipeline storage and digitization. It will be tested in a strong magnetic field in a beam containing electrons, hadrons and muons.

1. INTRODUCTION

High luminosity and high multiplicities in a high-level radiation environment will characterize the operation of LHC and challenge the performance of the detectors. To face these exceptional experimental conditions, silicon detectors look very attractive for calorimeter applications: they allow flexible construction, fine granularity and fast charge collection. They work in high magnetic fields and have good radiation resistance. Examples of future applications are preshower based on silicon detectors proposed for LHC [1] and for the DELPHI upgrade at LEP. A position detector made of 2 mm silicon strips is being considered for a CeF_3 crystal calorimeter at LHC [2]. In these applications the active silicon surface area is of order 100 m^2 and cost starts to be a limiting issue.

In view of a large calorimeter for a LHC experiment, this proposal addresses both the cost of silicon detectors and the readout layout.

In projects for a LHC detector, often boundary constraints given by magnet and subdetectors dimensions impose a compact calorimeter. Among all possible choices for the active element in a sampling calorimeter, the silicon technology probably offers the most compact solution today. In this view we point out the following advantages:

1. Thickness of active layer. The silicon detector itself is less than 1/2 mm thick and with the preamplifier reaches a thickness of approximately 2 mm. One of the purposes of this proposal is to design a realistic active layer of minimum thickness.

2. Transverse segmentation. Silicon is far superior to other techniques and limited only by practical considerations of channel numbers. In a calorimeter of limited outer radius, occupancy, shower dimensions and therefore density and granularity play a major role. Technical problems as interconnections of detectors, number of preamplifier and read-out channels, noise, heat dissipation are issues to solve for a realistic design. This proposal addresses also these questions.

The Dubna R&D program aiming at large scale application of cheap silicon detectors in collaboration with Russian industry [3] opens up the possibility of building full calorimeter systems based on active silicon areas of order 1000 m^2. With active layer thicknesses of 400 μm sensitive to single mip, silicon instrumented calorimeters can be made most compact. The silicon technique allows to consider a very large number of readout channels. A compact hadron calorimeter with modest energy resolution (about 20 sampling planes), but with very good lateral and longitudinal segmentation is very attractive in LHC applications, where energy resolution is not a priority. A very good segmentation transforms the hadron calorimeter into a tracking calorimeter. With good lateral and longitudinal segmentation one can follow isolated muons through the hadron calorimeter. A few silicon planes can even be included in the muon trigger system, thanks to the fast response and the mip sensitivity of the silicon detector. In fact this might be the only way to trigger on low P_T isolated muon pairs coming from J/ψ or Upsilon decays in the case of heavy ion collisions. With good longitudinal segmentation one can control the development of hadronic showers and hence tag or correct false missing energy measurements. Longitudinal energy readouts can be added with different weights to correct for non-compensation effects, though silicon calorimeters can be built as compensating calorimeters [4]-[5]. Finally we note that for hadron calorimeters neutron fluences are reduced by an order of magnitude, since they are shielded by the electromagnetic calorimeters in front. Up to pseudorapidities of about 3 one expects neutron fluences in hadron calorimeters not to exceed 10^{13} n/cm^2 per year.

Extensive studies have been carried out on the radiation resistance of silicon detectors The various and independent investigations (see radiation damage studies on silicon detectors presented at Tuscaloosa (March 89), Como (June 90), Aachen (October 90), Fort Worth (October 90), ORNL (February 91), Florence (July 91), Minsk (October 91)) show that the detectors have good radiation resistance. The charge collection is not reduced more than 10% (for about 10 ns integrated signals) at 5×10^{13} n/cm^2. The C vs V detector characteristics show that a 400 μm thick detector can be operated at full depletion at a voltage definitively lower than 300 V after an irradiation of 5×10^{13} n/cm^2. The increase of leakage current with the neutron fluence affects only slightly the signal to noise ratio for a mip [6], when fast VLSI electronics (with 20 ns RC-CR shaping time) is used.

The proposed engineered full scale silicon hadron calorimeter will use the newly developed low cost detectors and VLSI electronics located on the silicon mosaic supporting structure. Since one year, a development program has been started together with ELMA. The cost reduction is such that a ratio close to 1 is expected between processing cost and bulk silicon cost. At present, the processing cost is overwhelming the bulk silicon cost by a large factor. The development of fast (about 7 ns rise time) VLSI readout electronics [7]-[8] allows, once mounted on thin chip carriers, to be located on the silicon mosaics supporting structure. In a calorimeter, a minitower structure can be realized by summing the signals coming from preamplifiers, which readout a stack of silicon detectors along the longitudinal direction. The circuit for the minitower longitudinal sum was designed and tested [8]-[9]. So far, the VLSI electronics has shown to be resistant in the range of neutron fluences investigated (approximately $1\text{-}2 \times 10^{13}$ n/cm^2). No MOS component are envisaged in the coming preamplifier version to improve its resistance to gamma radiation. The development of a new radiation resistance VLSI preamplifier version is carried on in the SICAPO program.

2. MECHANICAL LAYOUT

The size and the organization of the test module are an approximation of one module of a typical hadron calorimeter of an experiment for LHC.

The module has a square constant cross section, because a tapered shape depends on the design of the experiment and in any case does not affect the test (fig.1).

All the electrical connections are concentrated in one side, while the cooling occupies an other side. These two sides are maintained separated in the test module to allow an easier access to the electronics, but the two functions could be arranged on the same side in the real calorimeter. This arrangement of the output allows a straightforward extrapolation of the organization of the test module to a real calorimeter whose modules should be 2 or 4 times larger in cross section. The active cross section of the test module will be 48x48 cm^2, enough to assure the full lateral containment of the hadronic shower.

The total thickness of the test module is 8.5 interaction lengths (see in table 1 the detailed account), subdivided in 40 homogeneous sampling. Longitudinally they are organized in 10 segments of 2, 2, 2, 4, 5, 5, 5, 5, 5, 5 layers; this redundant grouping will allow to optimize the grouping in a real calorimeter.

The absorber plates are constituted by 7 mm of Pb followed by 18 mm of Cu and sandwiched between two sheets of Cu of 2 and 5 mm. The Cu sheets are introduced to improve the flatness and roughness characteristics of the plate and to transmit outside the heat produced in the contiguous active plane (fig.2); their thickness guaranties a temperature gradient of less than 1^0C on the whole cross surface of the module when the average heat dissipation on the active plane is 40 w/m^2 (see later). The combination of the appropriate thicknesses of Pb and Cu (because copper and iron have similar values of the critical energy) will assure the compensation according to what it is discussed in the appendix 7.1

The active plane contains the silicon diodes sandwiched between two rigid circuit boards; on one of them are mounted the preamplifiers lodged in holes of a sheet of polyethylene envisaged to moderate neutrons in a real LHC calorimeter, the whole layer is closed by a third rigid board for mechanical protection (see fig 3). The total thickness of the active plane is 2.9 mm. A heat conducting sheet will be added to help the heat exchange in the 3.5 mm gap foreseen between the absorber plates. With this structure the local temperature gradient on the silicon diodes is less than 1^0C (Fig. 4)

At the end of each longitudinal segment, the gap between the absorber plates will be 8 mm wide to allocate also one service plane carrying the HV distribution to the segment, the summing of the signal from the active planes of the segment to form minitowers, the pipelining of their output and the controls.

Each plane contains 576 silicon detectors, 2x2 cm^2 in area; a preamplifier amplifies the signal coming from a pad of 4x4 cm^2 formed by 4 adjacent detectors (there are indeed 144 pads per plane). On the service plane the amplified signals coming from the pads occupying the same lateral position on the active planes of the same segment are summed to form a minitower signal (fig. 5).

For each segment the volume is indeed subdivided in 144 minitowers, and the volume of the whole calorimeter is subdivided in 1440 minitowers.

The layout of the test module is sketched in fig. 6, where are reported the main dimensions and few details.

Before beginning the mass production of the active planes for the test module, it will be assembled a small electromagnetic calorimeter in order to gain confidence in the whole project.

The test module will be tested on the beam either alone or following either the small silicon electromagnetic calorimeter or a matrix of CeF_3 crystals. In order to improve the granularity for electromagnetic showers of the test module, when it is used alone, each of the four minitowers of its first four segments around the central axis are further subdivided in four towers 2x2 cm^2 in section. Therefore additional 48 minitowers (64 minitowers are replacing the expected 16 minitowers of the central region of the electromagnetic section) are added to the 1440 accounted above, giving a total of 1488 minitowers to be read out.

3. ELECTRONICS LAYOUT

3.1 FRONT-END ELECTRONICS AND LONGITUDINAL MINITOWERS

The VLSI read-out is organized as shown in fig.7. Each pad of the stack, whose active area is 16 cm^2, is coupled to a monolithic Charge Sensitive Preamplifier (CSP). The preamplifier outputs are all summed and shaped with a 20 nsec RC-CR filter. Every analogical sum is equivalent to the shunting of detectors. The advantage of this solution is modularity and feasibility in the integration : both the CSP and the shaper are built with the same monolithic design and the CSP must match only one kind of detector. The number of detectors composing the stack can be varied, as required by the calorimeter organization, but the matching of the whole stack to the CSP is always satisfied.

Fig.8 shows a card (designed and built by the SICAPO collaboration) to readout a minitower of an electromagnetic Si/W calorimeter [9], using the V1 version of the VLSI preamplifier, made by SGS-THOMSON [7]. Each V1 preamplifier is coupled to two 2 x 2 cm^2 active area and 395 μm thick fully depleted Si detectors, located along the beam direction (the overall input detector capacitance is 208 pF). The adder circuit, fig. 8, is used to sum and shape the output signals from 4 subsequent preamplifiers along the beam direction. This corresponds to sum the energy deposited and sensed by 8 subsequent detectors.

Fig. 9 shows the pedestal noise distribution of a muon particle traversing a calorimeter cell. The most probable energy loss of the muon particle is 1.044 ± 0.015 MeV. This value is well in agreement with the one expected for a mip traversing a 3.16 mm thick silicon absorber (i. e. 8 fully depleted Si detectors). The standard deviation of the pedestal noise distribution is 160 ± 5 keV, corresponding to a single preamplifier noise of about 80 keV. This latest value is well in agreement with the one expected for the version V1, when the input capacitance is about 208 pF and the RC-CR shaping time of 20 nsec is used [7].

A new improved version (V2) of the CSP is built, by using (as for the V1 version) npn input transistors and the HF2CMOS technology. Its main feature is a very low series noise, with a base spreading resistance of about 14 Ω [9]. At 20 nsec RC-CR shaping time and for 104 pF input resistance (equivalent to one 2 x 2 cm^2 active area and 395 μm thick fully depleted Si detector), the measured value of the Equivalent Noise Charge (ENC) is 3800 electrons. For a 395 μm thick and 16 cm^2 active area Si detector, the ENC value is about 10400 electrons (equivalent to about 37 keV). The power dissipation is about 40 mW per CSP when the maximum output swing of 5 V is required, but the default value is only about 10mW, when operated to a reduced dynamic range.

Every CSP is able to drive a 50 Ω coaxial cable terminated at both ends. The non-linerarity curve at the receiving end of a terminated coaxial cable (where the signal is 1/2 the CSP output) is shown in fig. 10 : for a 5 V output swing (for the full output) the linearity is within 0.8%. The expected ENC value for a minitower of 5 subsequent 395 μm thick and 16 16 cm^2 active area fully depleted Si detectors is about 84 keV. The expected most probable energy loss of a muon particle is about 640 keV. Thus the signal to noise ratio for a mip is about 8 to 1 (for a minitower of 2 subsequent Si detectors the signal to noise ratio is about 5 to 1).

The monolithic layout is shown in fig. 11. For this application, a version of this preamplifier will be fabricated in integrated chips containing 4 channels each. The chips will be organized as CSP and shapers depending on the preamplifier network employed.

3.2 ANALOG PIPELINE FOR THE HADRONIC SILICON CALORIMETER

Low power custom VLSI analog memories operating in pipeline mode are good candidates to locally store pulse height of silicon detector signals. This consideration is particularly true in the case of a silicon calorimeter at LHC with a few hundred of thousands electronic channels on the detector.

Previous studies on the analog memory technique utilizing silicon CMOS technology for DRDC project RD2 (SITP detector) have demonstrated the basic functionality of the analog memory principle in a 4 channel prototype chip [10]. A more complete readout architecture has been also implemented in a 32 channel analog memory chip [11]. In this prototype the full functionality required at LHC operating conditions has been successfully tested. The chip performs 1 μsec local storage with a writing speed of 67 MHz, readout of memory columns selected by the level 1 trigger and provides analog multiplexed output signals ready to be digitized.

Preliminary measurements of those chips indicate a dynamic range of 10 to 11 bit. To cover the dynamic range of 16 bit of the silicon hadronic calorimeter, a good approach is to combine two parallel analog memories with different gains.

By implementing an attenuator in front of the pipeline input (50 to 100 Ω input resistance), a preliminary test with the existing 4 channel chip will be performed. This attenuation can be used for dynamic range adapting and can set different gain factors for the two pipeline channels. The CERN Electronic group will implement the necessary modifications to the analog memory for the final test.

The charge sampling technique, by which the input signal is integrated over the clock period and implemented in these analog pipeline prototypes, is very attractive. It is insensitive to timing jitter and needs no further signal processing before or after digitization, but simple summation of contiguous samples.

4. SILICON DETECTORS PROCUREMENT

We are requesting the silicon detectors from Russia. The Joint Institute for Nuclear Research (Dubna) is coordinating this effort. The total surface of detectors required for a LHC hadron calorimeter is approximately 3.10^7 cm^2. At present, the manufacturing process cost dominates the overall cost of silicon detectors. The present cost of raw silicon wafers (100 mm diameter of Wacker material), corresponds to approximately 0.9 SFr / cm^2, assuming 70% production yield and the usage of about 60-65% of the available wafer area. A large quantity order, a better usage of the available wafer area and an increase up to 80% of the production yield could bring the cost of ingots to the level of 0.6 SFr / cm^2.

In close collaboration with industry and applied research physics groups, we want to develop a technology of detectors production which combines industrial mass production where the quality control is performed at every production step. This collaboration makes it possible to optimize the production and test procedure according to our specification and should result in considerable cost reduction. The goal is to reduce the cost of the detector fabrication process in Russia to the level of the cost of raw silicon ingots. This program has been undertaken since 1989 by JINR (Dubna) in collaboration with Research and Production Association ELMA (Zelenograd, Moscow region, Russia) and other interested groups of physicists from West Europe and USA.

ELMA has all the facilities for large scale production of silicon detectors, such as wafer processing (slicing, lapping, polishing), photolythography, thermodiffusion, oxide growth, implantation etc. Employees have the proper professional level. ELMA is the main producer of the silicon substrata for microelectronics in the RSFSR.

At the same time the program involves also the facilities which were constructed at Dubna having a total area of 350 m^2 and a clean area of 70 m^2, where the major steps of the planar technology such as thermodiffusion, thermal oxidation growth, implantation, photolythography and metal deposition can be carried out.

The first phase of the program was completed in 1991. It resulted in creating a specialized technology and in a successful fabrication at ELMA of several hundreds detectors using Wacker float zone refined silicon. The projected cost for n-type Silicon detectors with 4 kΩ.cm resistivity is 0.6 SFr / cm^2, assuming a production of > 10 tons. The topology of the detector is shown in fig.12. The sensitive area is 2 cm x 2 cm, the thickness 400μm.

For all samples the depletion voltage does not exceed 80 V. Fig. 13 shows the histogram of leakage currents of the fully depleted detectors at 80 V, measured at Dubna just after production. The same distribution measured one month in the INFN-Milan laboratory is shown in fig.14.

As can be seen from these figures, all the detectors can be accepted for a calorimeter. Comparison of these figures gives also an indication of the stability of the leakage current of a detector.

One of the major goals of this proposal is to produce approximately 10 m^2 of the detectors using the same technology and in parallel to continue the technology improvement program at ELMA aimed to further reduction of the production cost of silicon detectors to be used at LHC.

5. DATA TAKING AND BEAM TIME REQUIREMENTS

It is foreseen to install and test the hadron calorimeter module in the gap of the 3 Tesla EHS magnet in the H2 beam line. We will benefit of the infrastructure of the RD5 set-up, which is considered a mandatory prerequisite.

The data acquisition comprises 1488 minitowers in addition to the chamber and beam counter readout of the RD5 set-up.

In order to run the front-end synchronously at LHC speeds a powerful first level trigger would have to be provided. Be it a real trigger processor or a smaller device simulating its decisions the consequence for the data acquisition remains the same. Approximately 1500 16-bit words come at a rate defined primarily by the acquisition time. This number does not change by using different types of ADC's. The acquisition time will be ≈1ms which is the time necessary to transfer the digitized events out of the ADC's environment.

The data acquisition of RD5 is presently capable of running at a very moderate but cost effective 0.5Mbyte/s which is considered adequate for the amount of data required for testing the silicon calorimeter. The RD5 upgrade foresees a number of 68020 CPU's mainly for zero suppression and second level trigger tasks, mainly for the RD5 tracking calorimeter equipped with 5000 channels of honeycomb chambers. By the time the silicon calorimeter will arrive the complete readout chain of the tracking calorimeter will become available. No particular difficulties should be encountered on the digital side when connecting the silicon calorimeter.

Matching of analogue signals, however, strongly depends on the ADC-system. There is the choice between two existing systems, one of which is used successfully for the tracking calorimeter's honeycomb chambers. In case pulse shaping is not possible to the extent and accuracy desired, a commercially produced ADC-system with some 1600 12bit charge sensitive channels is also available.

All preamplifier outputs will be read at a speed of 66 MHz. An analogue pipeline will be employed in order to store data during an assumed first level trigger running time. So far the analogue chain is able to undertake 64 pipelining steps. A time of max 1μs may elapse prior to the trigger decision.

For 1993 we require 3 weeks for setting-up, calibration and test. The 1994 data taking will be organized as outlined in the planning below:

Energy	magnet	run type	time	comments
various	on/off		150 h	beam/exp./trig. setup
10 GeV	off	π/μ/e	75 h	5 scan conditions
30 GeV	off	π/μ/e	75 h	5 scan conditions
100 GeV	off	π/μ/e	75 h	5 scan conditions
300 GeV	off	π/μ/e	75 h	5 scan conditions
10 GeV	on	π/μ/e	75 h	5 scan conditions
30 GeV	on	π/μ/e	75 h	5 scan conditions
100 GeV	on	π/μ/e	75 h	5 scan conditions
300 GeV	on	π/μ/e	75 h	5 scan conditions
TOTAL			**750 h**	**≈30 d**

6. TIME SCHEDULE AND BUDGET

Steps of the design and construction are outlined below. By end of 1994 we aim to have a full understanding of engineering, technical and instrumental aspects in order to select this technology for a LHC experiment.

1992 Start of fabrication of detectors.
Definition of preamp/pipeline integration.
Start of construction of read out channels.
Prototypes of supporting structures.
Test of detectors.
Assembly of electromagnetic calorimeter.
Design and construction of hadron calorimeter mechanical structure.
Design of active plane.

1993 Completion of detector fabrication and test.
Completion of read out electronics.
Fabrication of active planes.
Assembly of hadron calorimeter.
Installation on test beam.
Initial test on beam.

1994 Final test beam measurements.

Table 2 shows budget estimate and sources of funding. Approval of Funding Agencies has to be obtained. Table 3 describes sharing of responsibilities among the participating Institutions.

7) COMPUTING

We foresee to write of order 100 cassettes in 1993 and 200 cassettes in 1994. The estimated off-line computing need on the CERN computers for data analysis is of order 1000 hours (CERN units) for 1993 and 1994. The simulation will be done on workstations.

8) APPENDICES

8.1 COMPENSATION

Obtaining a linear response to the energy of incoming particles and jets and an optimized energy resolution necessitates the achievement of the compensation (or the quasi-compensation) condition, namely e/π about 1. Contrary to the electromagnetic cascading, which is fully described by QED and depends essentially on the density of electrons in the absorber medium, the hadronic cascade is propagated by a variety of complex hadronic processes [14]-[16]. Decays of hadronic resonances created during the degradation of the energy of the incident hadrons and charge exchange reactions in these processes, yield an electromagnetic component of any hadronic shower; this component is largely determined by the production of pions in the first interactions, and therefore event-by-event fluctuations are important. In the hadronic interactions of a cascade, a sizeable amount of the available energy is converted into excitation or break-up of the absorber nuclei, of which only a fraction would result in visible energy. The performance of hadron calorimeters is determined by the relative response of the electromagnetic and non-electromagnetic shower component, namely the e/π ratio [17].

The e/π ratio can be written as:

$$e/\pi = (e/mip)/[(e/mip)\, f_{em} + (h/mip)\,(1-f_{em})]$$

where f_{em} is the average fraction of the converted electromagnetic energy produced by the hadron cascade (a detailed discussion of this equation is in [17] and [18]). The logarithmic increase of f_{em} [12] with the energy of the incoming hadron results in a signal ratio e/π, which is also energy dependent if (as generally occurs) $e/mip \neq h/mip$. However, if $e/\pi=1$, the values of e/mip and h/mip are equal, independently of f_{em}.

The visible energy of a hadronic shower, $\varepsilon_{vis}(\pi)$, can be expressed as [5]:

$$\varepsilon_{vis}(\pi)=E\cdot F(Si)\,[h/mip + f_{em}\,(e/mip-h/mip)]$$

where E is the energy of the incoming hadron, F(Si) is the fraction of the incoming energy deposited by a minimum ionizing particle in the silicon detectors. The equation shows that it is only in the situation where e/mip = h/mip (i.e. $e/\pi=1$, the so called compensation condition) that the calorimeter response is proportional to the incoming energy E, independently of f_{em}.

Furthermore, the energy resolution [15] of the calorimeter is minimized and becomes proportional to $1/(E)^{1/2}$.

In a silicon hadronic calorimeter, in which the passive absorbers are made of low and high Z material as Fe and Pb plates, the equalization of the electromagnetic and hadronic signals [5] can be achieved. The combination of Pb and Fe leads to an electromagnetic shower energy transformation effect, generated by a sharp transition from small to large values of the critical energy (ε_{cr}=7.4 MeV and 21.0 MeV for Pb and Fe, respectively). Because the value of ε_{cr} coincides with that value of the electron energy below which the ionization energy loss starts to dominate the energy loss by bremsstrahlung, the increase of the the critical energy of the absorber favours the ionization energy loss with respect to the energy loss by radiation. The energy spectra of the incident electrons becomes softer when moving from a high-Z (Pb) absorber to a low-Z (Fe) absorber. The low-Z (Fe) part of the absorber produces a filtering effect [19] on the electrons. As a result, the energy of the shower is transformed and the response of the calorimeter to the incoming electromagnetic shower is modified.

A hadron Si/(Fe,Pb) calorimeter, consisting of 30 sets of absorbers (made of Pb and Fe plates) interspersed with silicon readout mosaics, has been put into operation by SICAPO collaboration. In each sampling the thickness of Pb and Fe are kept constant as well as the respective positions of the absorber plates. Each set of absorbers is 23 mm thick. The total calorimeter depth is about 4.6 λ, taking into account the supporting structures of the silicon mosaics. Each silicon mosaics consists of 400 silicon detectors of 2x2 cm^2 active area. The calorimeter is equipped by 12000 detectors. The data have been taken in the T9 beam at the CERN-PS. The incoming electron and hadron energies were 6, 8, 10 and 12 GeV. Sets of data were taken with absorber plates, in each sampling, of 23 mm Fe, 3 mm Pb and 20 mm Fe, 8 mm Pb and 15 mm Fe, 13 mm Pb and 10 mm Fe. The experimental data show that the compensation condition is achieved in a PbFe-Si-PbFe calorimeter configuration (along the beam direction), when 5.4 ± 1.0 mm of Pb are used [5].

8.2 NEUTRON RADIATION HARDNESS

The radiation resistance of silicon detectors and associated electronics have been analyzed at the Workshops and Conferences: Tuscaloosa (89), Como (90), Aachen (90), Fort Worth (90), ORNL (91), Florence (91), Minsk (91). Of main concern [20] for the detectors is the high flux of albedo neutrons generated in the experimental cavities for which a fluence of about 10^{13} neutrons per cm^2 has been calculated for a Pb calorimeter environment at LHC [21] for rapidities ≤ 2, at luminosity of 10^{34} $cm^{-2}s^{-1}$ and during 10^7 seconds (an operational year for LHC), when no polyethylene moderator is located next to the silicon detectors. Extensive measurements of the damages induced in silicon detectors by neutrons of about 1 MeV have been started by many experimental groups and the main consequences for a calorimeter operation are summarized here.

The neutrons create defect states in the silicon volume acting as generation-recombination centers decreasing the minority carrier life time; as a consequence the diode reverse current I_r is increasing linearly with the neutron fluence Φ:

$$I_r - I_{ro} = \alpha \Phi V$$

where V is the detector volume and α the damage coefficient. Including the self annealing effect at room temperature, the value of α has been found to be 4.5-6 x 10^{-17} A cm^{-1} at 20^oC for irradiation up to 10^{14} n cm^{-2} [6], [22]. Consequently a 400 μm thick detector irradiated at 10^{13} n cm^{-2} has a reverse current of about 20 μA cm^{-2}, which has to be sustained by the front end electronics. It has been measured [6], using the V1 version of the monolithic preamplifier described in the electronic chapter, that the Equivalent Noise Charge is degraded by no more than 5 % at least up to 100 μA.

The neutron induced defects in the silicon bulk create charge centers acting as acceptors modifying the doping concentration of the initial material. The C vs V detector characteristics show that a 400 μm thick detector can be operated at full depletion at a voltage definitively lower than 300 V after an irradiation of 5×10^{13} n/cm^2.

Finally the induced defects in the detector active volume act as trapping centers for the charge deposited by a minimum ionizing particle. However it has been measured up to a fluence of 5 x 10^{13} n cm^{-2} that the time development of the current signal response is not significantly degraded and that the charge collection deficiency is of the order of 10 % when integrating the signal over 10 ns. This deficiency could be reduced by using the envisaged 20 nsec shaping time.

REFERENCES

[1] R&D proposal on Si preshower, RD2

[2] R&D proposal on crystals, RD18

[3] The Dubna R&D effort on large scale application of si detectors.

[4] SICAPO collaboration, Evidence for the compensation condition in Si/U hadronic calorimetry by the local hardening effect, Phys. Lett. B 242 (1990), 243

[5] SICAPO collaboration, Evidence for compensation in (Fe,Pb) hadron calorimeter by the filtering effect, CERN-PPE/91-218 (November 91)

[6] E.Borchi et al., Nucl.Phys. B (Proc.Supp.) 23 A (1991), 352
E.Borchi et al., Proc. of ECFA LHC Workshop, CERN 90-10/ECFA 90-133, Vol III (3.12.90), 721

[7] A.Gola et al., Nucl. Instr. and Meth. Phys. Res. A 292 (1990), 648

[8] A.Gola et al., to be submitted to Nucl. Instr. and Meth. Phys. Res.

[9] A.Gola et al., Nucl. Phys. B (Proc. Supp.) 23A (1991), 207

[10] P.Jarron et al., Analog sampling technique in CMOS technology, LeCroy Electronics for Particle Physics Conference 1991

[11] The status report to the DRDC of the RD2 collaboration, 14/01/1992

[12] U.Amaldi, Physica Scripta 23 (1981), 409

[13] J.Brau and T.A.Gabriel, Nucl Instr and Meth. A239 (1985), 489;
T.A.Gabriel et al. , IEEE Trans Nucl. Science NS-32 (1985), 1

[14] C.Leroy et al., Nucl. Instr. and Meth. A252 (1986), 4

[15] R.Wigmans, Nucl. Instr. and Meth. A259 (1987), 389

[16] J.E.Brau, T.Gabriel and P.G.Rancoita, Proc. of the summer study on High Energy in the 1990s (June 27- July 5, 1988), Snowmass, World Scient. Publ., Singapore (1989), Editor S.Jensen, p 824

[17] E.Borchi et al. (SICAPO coll.), CERN-PPE/91-18 (29.1.91), Nucl. Phys.B (Proc.Supp.) 23A (1991), 62

[18] E.Borchi, C.Leroy, P.G.Rancoita and A.Seidman, Proc. of the Symposium on Detector Research and Development for the SSC, Fort Worth (October 1990), World Scientific (1991), p 30

[19] E.Borchi et al. (SICAPO coll.), Phys.Lett.B222 (1989), 526

[20] G.Hall, Radiation resistance of semiconductors and associated electronics, Large Hadron Collider Workshop, CERN 90-10, Vol 3 (1990) 696.

[21] G.R.Stevenson, new dose calculations for LHC detectors, Large Hadron Collider Workshop, CERN 90-10,Vol 3 (1990) 566.

[22] F.Lemeilleur et al, Neutron-induced radiation damage in silicon detectors, CERN/ECP 91-21; C.Furetta (SICAPO coll.) , Radiation hardness in silicon detectors, talk presented at the Radiation Damage Florence Workshop (July 1991)

Table 1: STRUCTURE OF THE SILICON CALORIMETER TEST MODULE

1. ABSORBER PLANES CONSISTING OF GROUPS OF (Pb+Cu) PLATES:

a) 1 plate thickness:	Pb=7 mm (1.25 X_0 or 0.041 λ)
	Cu=25 mm (1.75 X_0 or 0.166 λ)
	Total=32 mm (3.0 X_0 or 0.207 λ)
b) lateral dimensions:	540 mm x 540 mm
c) total n. of planes:	40
d) total plate thickness:	128 cm (120 X_0 or 8.28 λ)

2. DETECTOR PLANES:

a) area covered by Si detectors:	480 mm x 480 mm
b) detector dimensions:	20 mm x 20 mm
c) n. of Si detectors per plane:	576
d) n. of detector planes:	40
e) total n. of Si detectors:	23040
f) lateral summing of detectors:	4
g) n. of quad-preamps. per plane:	36 (39 in the e.m. section)
h) total n. of quad-preamp.	1488
i) width of detector gaps:	3.5 mm

3. SERVICE PLANES:

a) n. of service planes:	10
b) positions of service planes:	after 2,2,2,4,5,5,5,5,5,5 absorber&detector planes
c) n. of summing ampl. per plane:	144 (156 in the e.m. section)
d) total n. of summing amplifiers:	1488 (372 quad-preamp. chips)
e) width of service gaps	8 mm

Table 2: BUDGET FOR THE YEARS 1992, 1993, 1994
(subject to approval by Funding Agencies)

ITEMS	1992 1 m^2 [KSF]	1993-94 10 m^2 [KSF]	TOTAL [KSF]	RESPONSABILITY
1) Silicon Ingots (100 kg)	130	0	130	CERN
2) Detectors a) R&D	*150	0	150	Dubna
b) production	50	100	150	CERN/Dubna
3) Electronics:				
a) Preamplifiers:				
CAD and Simulations	**200	**50	250	SGS-THOMSON
Tooling (mask, layout)	135	0	135	INFN
Preproduction 100 quads	90	0	90	INFN
Production 1000 quads	0	50	50	INFN
Production 1000 quads	0	30	30	INFN
b) Pipeline	30	50	80	CERN
c) Connections	0	50	50	CERN/INFN
d) Power supplies	0	40	40	INFN/Vienna
e) ADC's existing	0	0	0	CERN/Vienna
f) DAQ/Trigger	0	50	50	Vienna
4) Mosaic supporting structure:				
a) Preliminary design and system integration	**50	**30	80	Ansaldo
b) Prototypes	30	0	30	CERN/INFN
c) Components:				
Industrial design + software	170	0	170	INFN
Mechanical tools + equipment	0	40	40	INFN
2 industrialized prototypes	0	20	20	INFN
38 supporting structures	0	100	100	INFN
d) Assembly	0	*100	100	Dubna/INFN
5) Mechanics:				
a) Copper + Lead	20	30	50	CERN/Dubna
b) Support	20	30	50	CERN/Dubna
c) Assembly	0	*20	20	CERN/Dubna
6) Running costs	20	80	100	CERN/USA
7) Administration	20	80	100	CERN
TOTAL	1115	950	2065	

* in kind contribution and/or manpower from RSFSR
** in kind contribution and manpower

Table 3: SHARING OF RESPONSABILITIES

ITEMS	RESPONSABILITY
1) Detectors :	
a) Development	Dubna
b) Bulk Silicon	CERN/Dubna/INFN
c) Production	Dubna
d) Quality Control	Dubna/INFN
2) Electronics:	
a) Front end development	INFN*
b) Production + tests	INFN*
c) Pipeline development + prod.	CERN/Dubna/Vienna
d) DAQ/Trigger	Dubna/Vienna
3) Mosaics:	
a) Prototype design	CERN/Dubna/INFN**/USA
b) Industrial design	INFN**
c) Prod. of supporting structures	INFN**
d) Assembly	Dubna/INFN**
e) Test (assembled pieces)	CERN/Dubna/INFN/USA/Vienna
4) Mechanics :	
a) Design	CERN/Dubna/INFN**
b) Construction	CERN/Dubna
5) Beam installation	All
6) Simulations	CERN/Dubna/INFN

* in collaboration with SGS-THOMSON

** in collaboration with Ansaldo

FIGURE CAPTIONS

Fig. 1 Perspective view of the prototype calorimeter

Fig. 2 Schematic of heath flow from the preamplifiers to lateral plate.

Fig. 3 Stratigraphy of active plane: cross section showing the preamplifier.

Fig. 4 Isothermal lines in the active plane; a) top view of the plane between the preamplifier and the silicon detector; b) cross section of the active plane, the preamplifier is located in the leftmost part of the drawing.
Each isotherm corresponds to a step of 0.08°C

Fig. 5 Summing of signals in "minitowers"

Fig. 6 Layout of prototype calorimeter indicating dimensions and connections of detectors in detectors. The small rectangles indicates the quad preamp.

Fig. 7 Preamplifier array and shaper .

Fig. 8 Printed circuit board for summing 4 preamplifier output signals

Fig. 9 Pedestal noise distribution and deposited energy distribution of a μ particle traversing a calorimeter cell

Fig. 10 Preamplifier integral non linearity. In the 5V output swing the non linearity is within 0.8%, compatible with errors of measurements. The measurement was performed at the receiving end of a terminated coaxial cable where the signal is 1/2 of the preamp output.

Fig. 11 Photograph of the monolithic layout of the charge sensitive preamplifier.

Fig. 12 Si detector cross section

Fig. 13 Leakage current of fully depleted detectors measured in Dubna

Fig. 14 Leakage current of fully depleted detectors measured in INFN-Milan laboratory a month later.

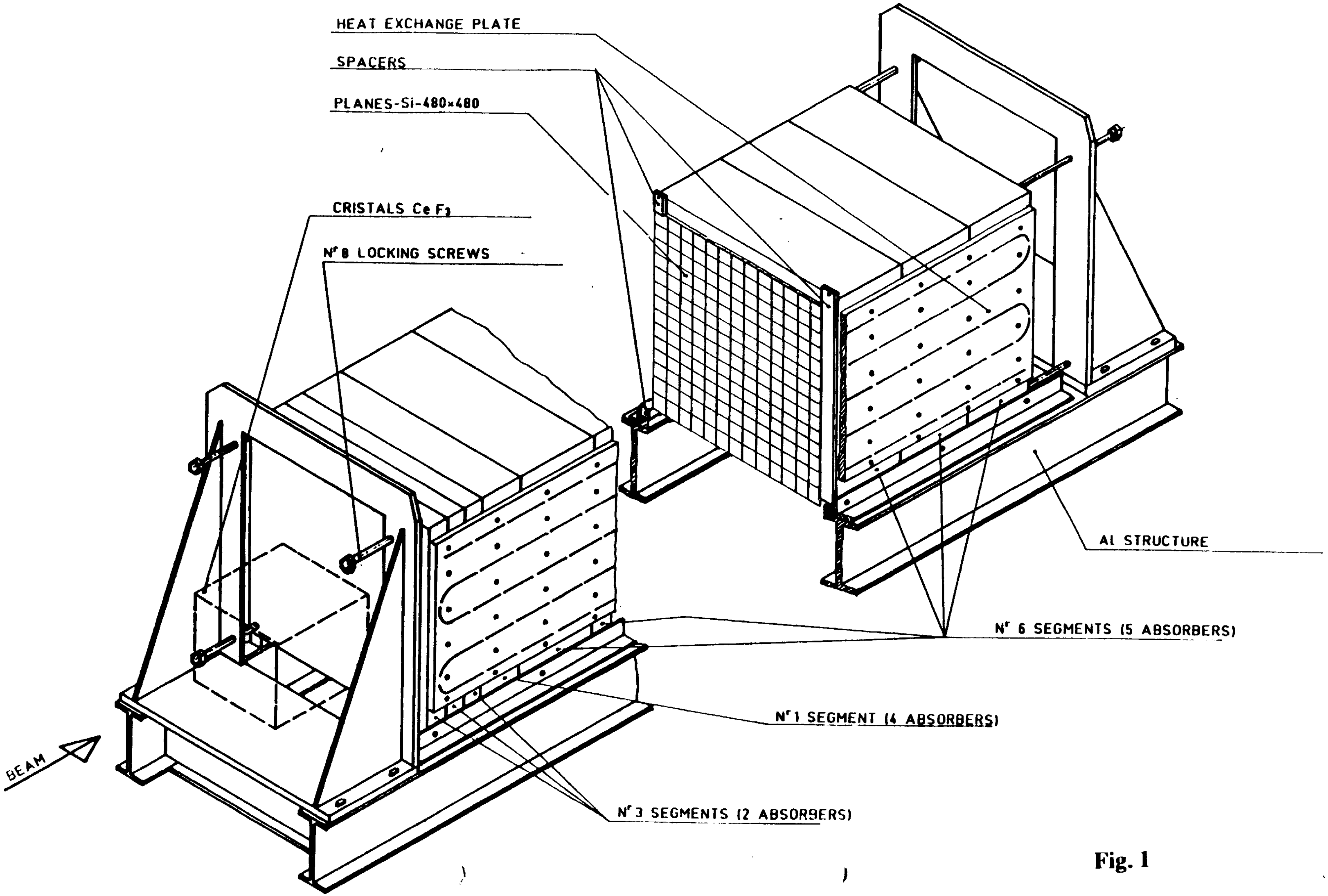
HEAT EXCHANGE PLATE
SPACERS
PLANES-Si-480×480
CRISTALS Ce F3
N°8 LOCKING SCREWS
Al STRUCTURE
N° 6 SEGMENTS (5 ABSORBERS)
N°1 SEGMENT (4 ABSORBERS)
N°3 SEGMENTS (2 ABSORBERS)
BEAM

Fig. 1

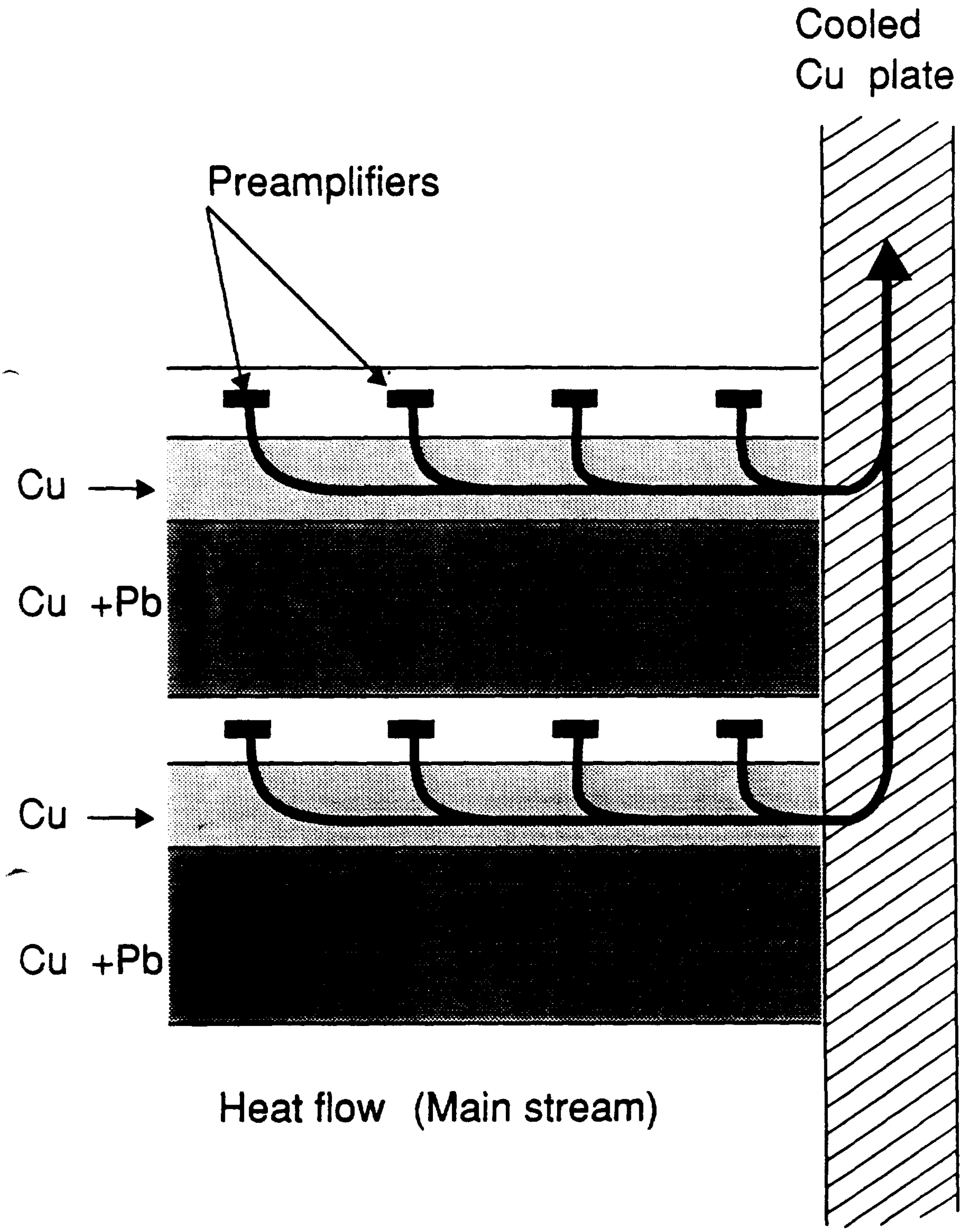
Cooled
Cu plate
Preamplifiers
Cu
Cu +Pb
Cu
Cu +Pb
Heat flow (Main stream)

Fig. 2

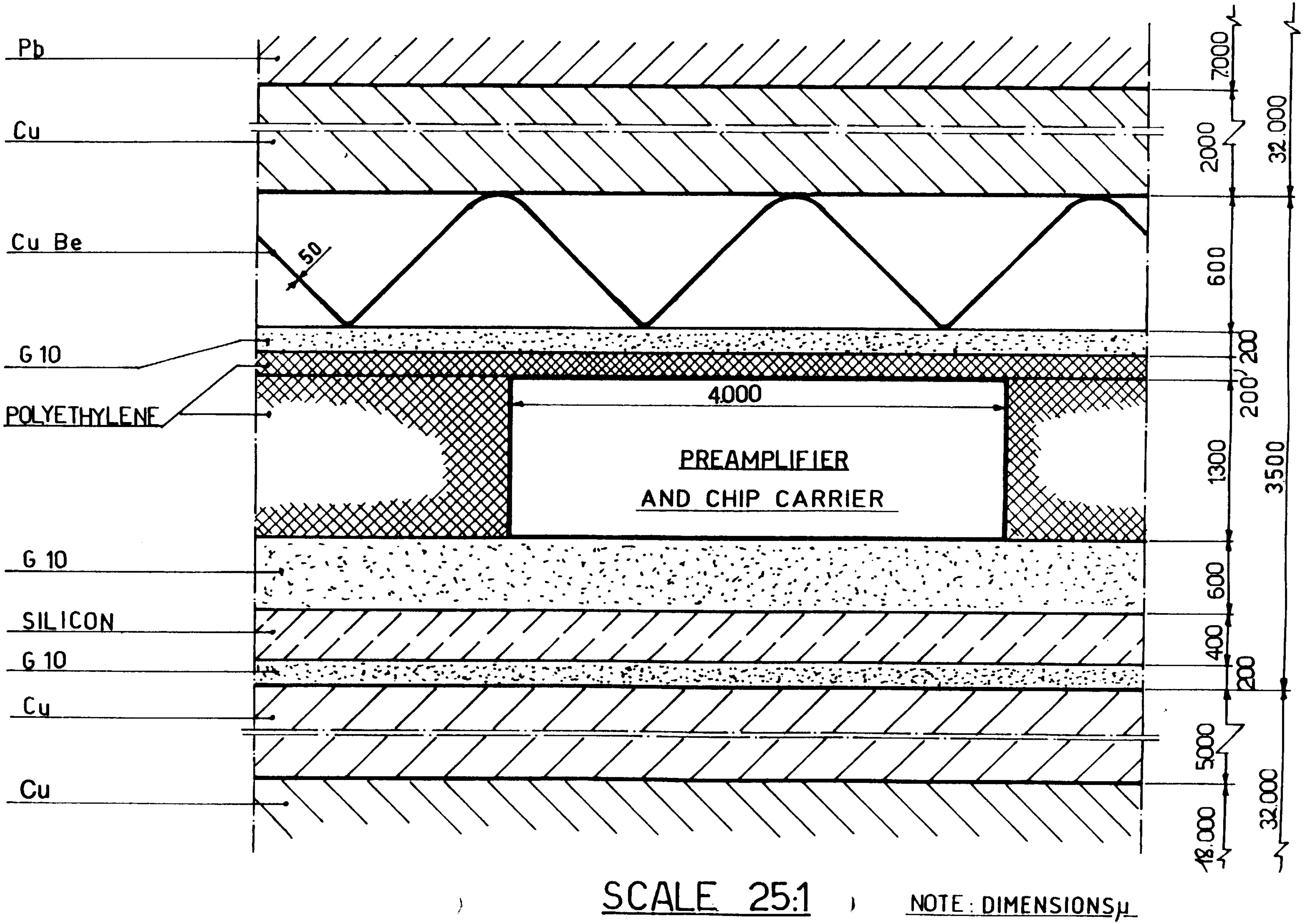

Pb
Cu
Cu Be
G 10
POLYETHYLENE
G 10
SILICON
G 10
Cu
Cu
50
4000
PREAMPLIFIER
AND CHIP CARRIER
7000
2000
600
200
200
1300
600
400
200
5000
18.000
32.000
3500
32.000
SCALE 25:1
NOTE : DIMENSIONS μ

Fig. 3

Fig. 4a

Fig. 4b

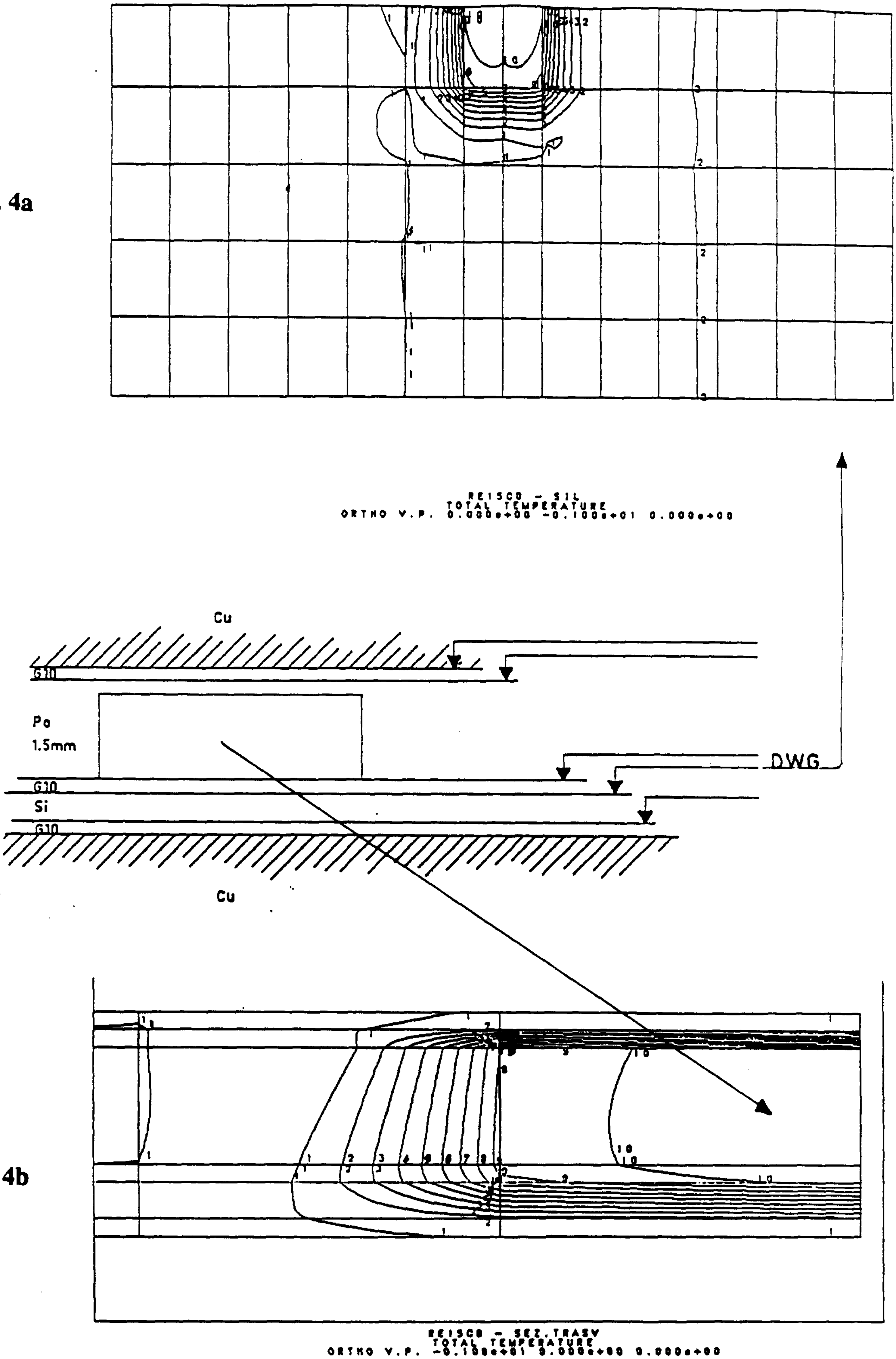
REISCO - SIL
TOTAL TEMPERATURE
ORTHO V.P. 0.000e+00 -0.100e+01 0.000e+00
Cu
G10
Po
1.5mm
G10
Si
G10
Cu
DWG
REISCO - SEZ.TRASV
TOTAL TEMPERATURE
ORTHO V.P. -0.108e+01 0.000e+00 0.000e+00

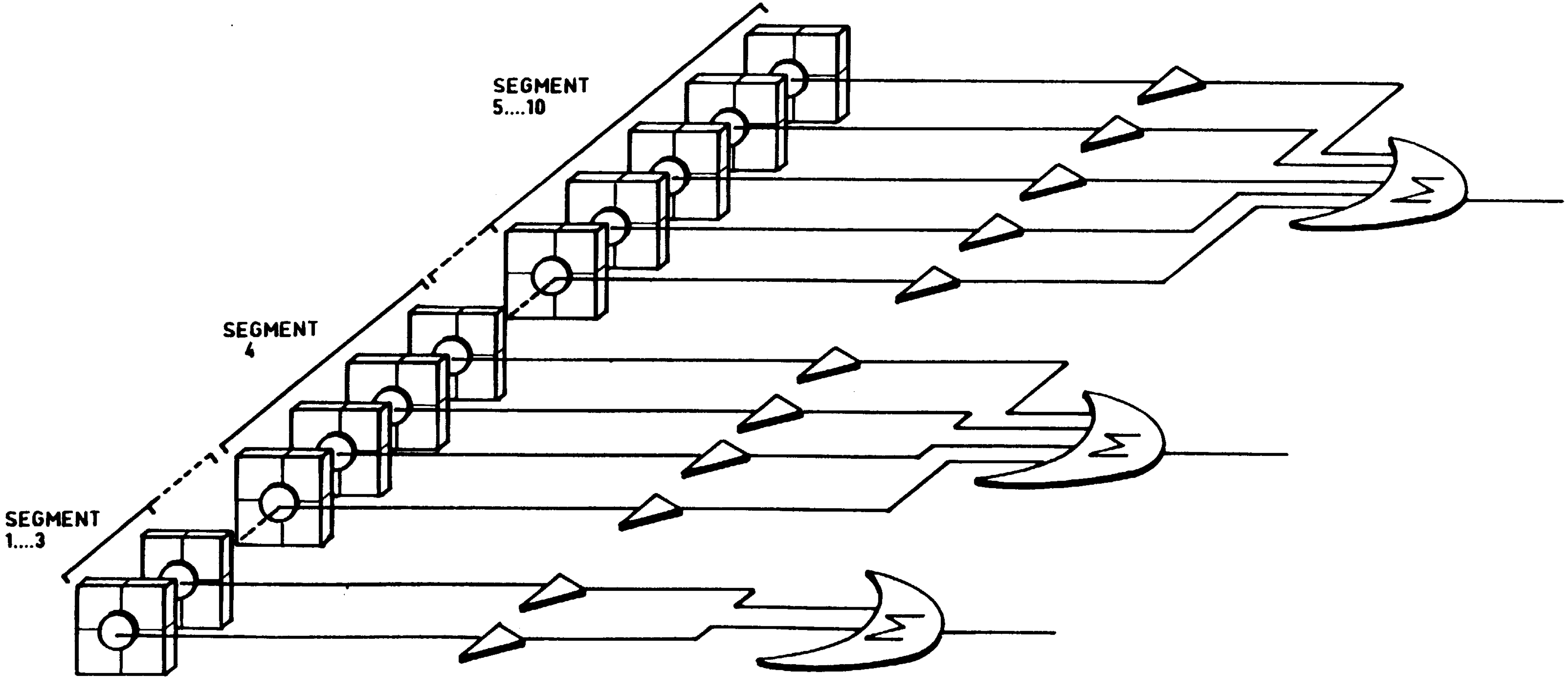

Fig. 5

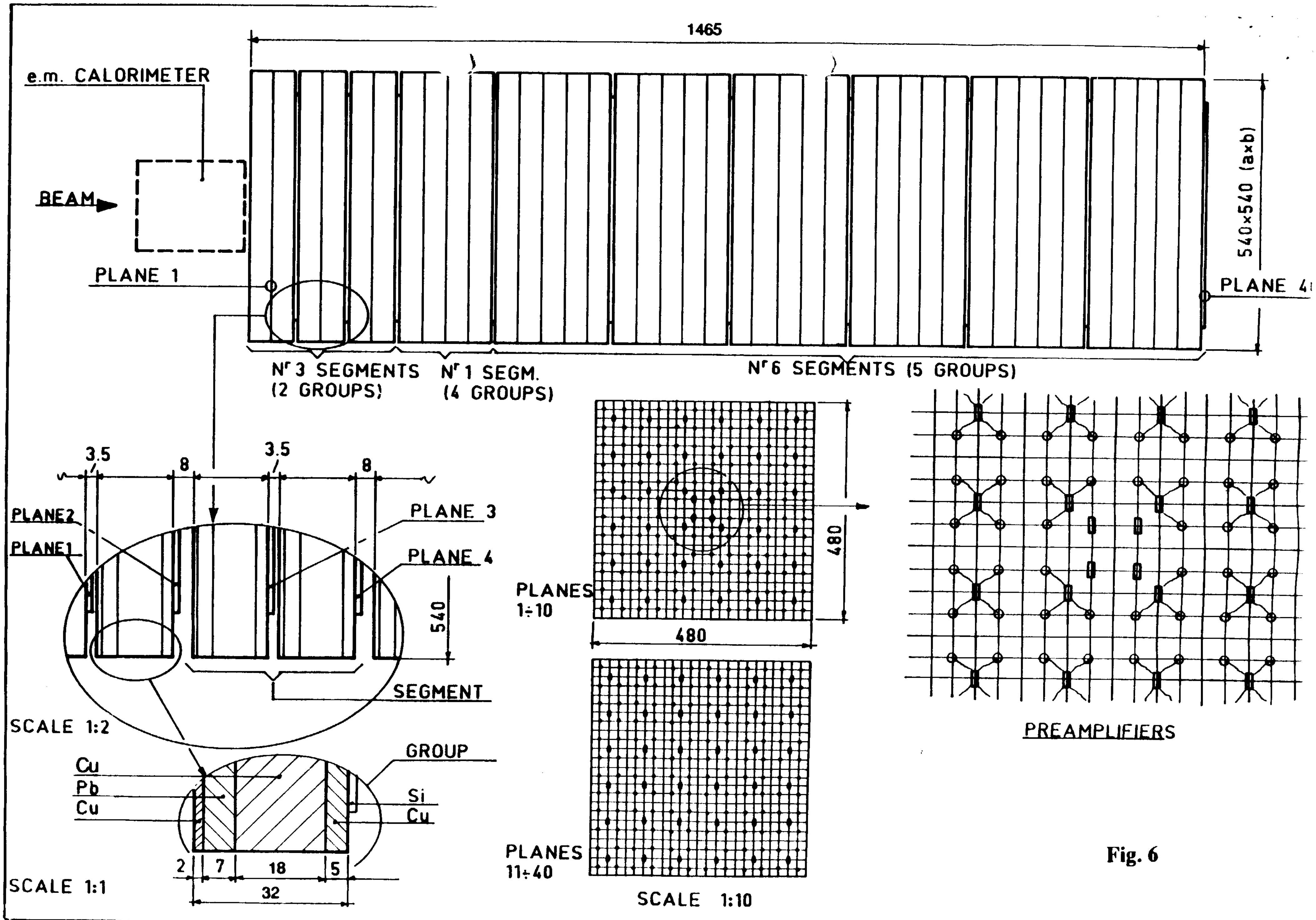
1465
e.m. CALORIMETER
BEAM
PLANE 1
PLANE 40
540×540 (a×b)
Nr 3 SEGMENTS
(2 GROUPS)
Nr 1 SEGM.
(4 GROUPS)
Nr 6 SEGMENTS (5 GROUPS)
3.5
8
3.5
8
PLANE2
PLANE1
PLANE 3
PLANE 4
540
SEGMENT
SCALE 1:2
GROUP
Cu
Pb
Cu
Si
Cu
2
7
18
5
32
SCALE 1:1
PLANES
1÷10
480
480
PLANES
11÷40
SCALE 1:10
PREAMPLIFIERS

Fig. 6

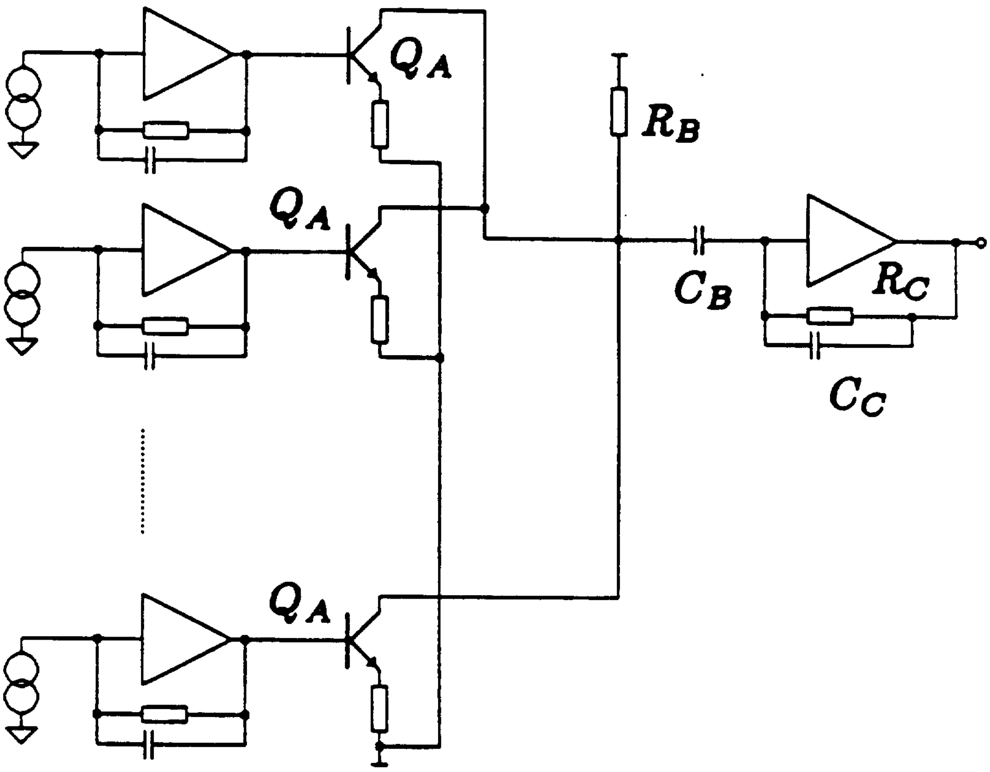

Fig. 7

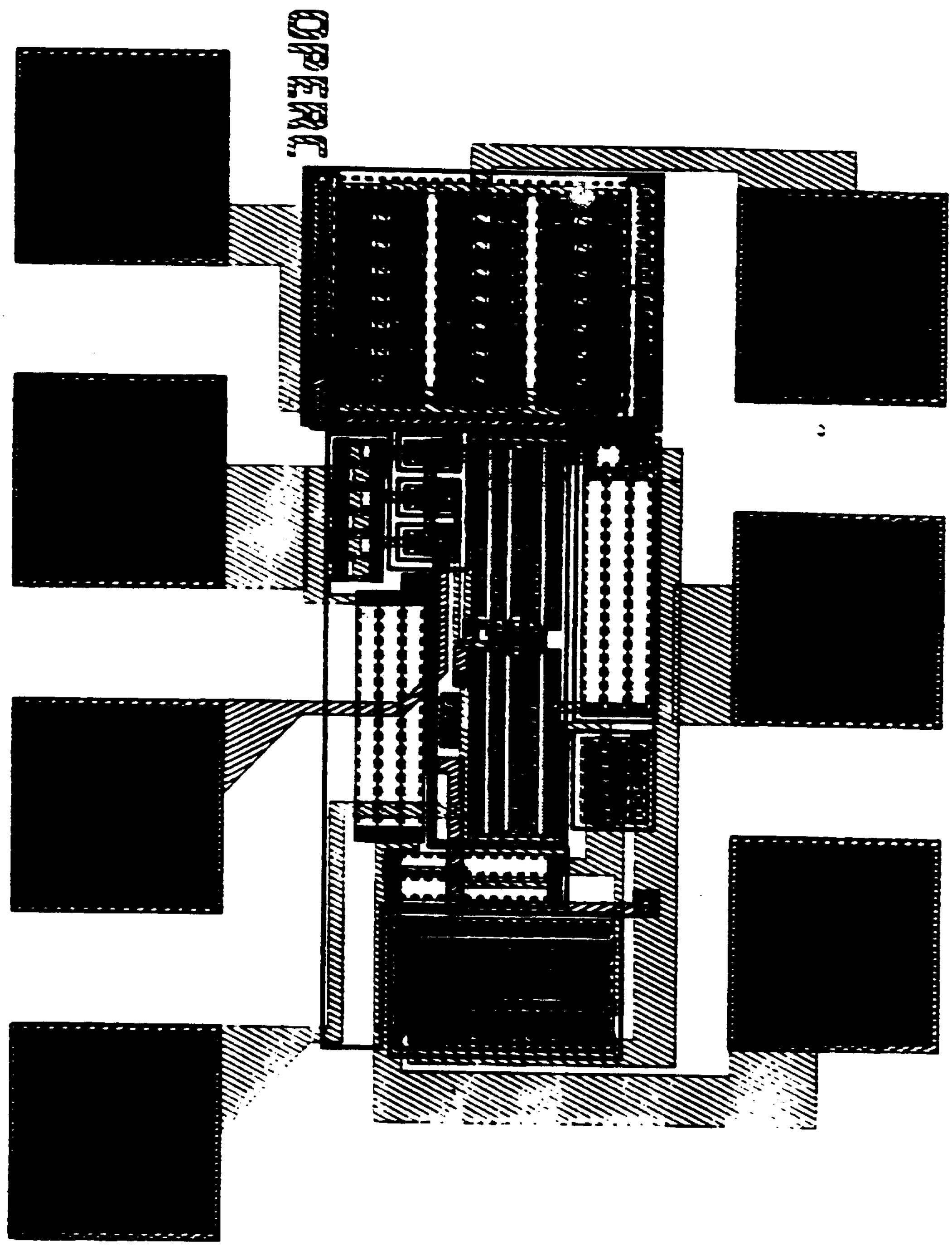

Fig. 8

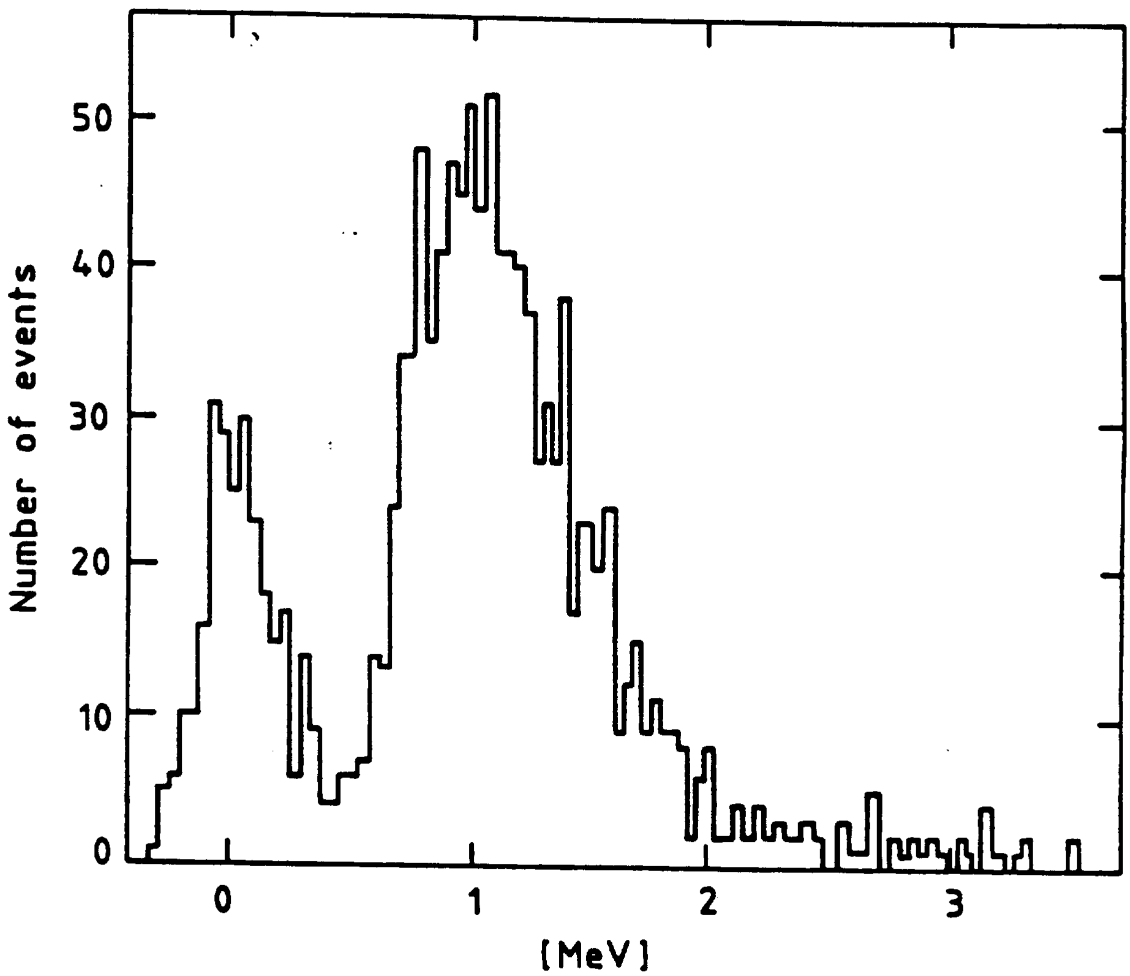

Fig. 9

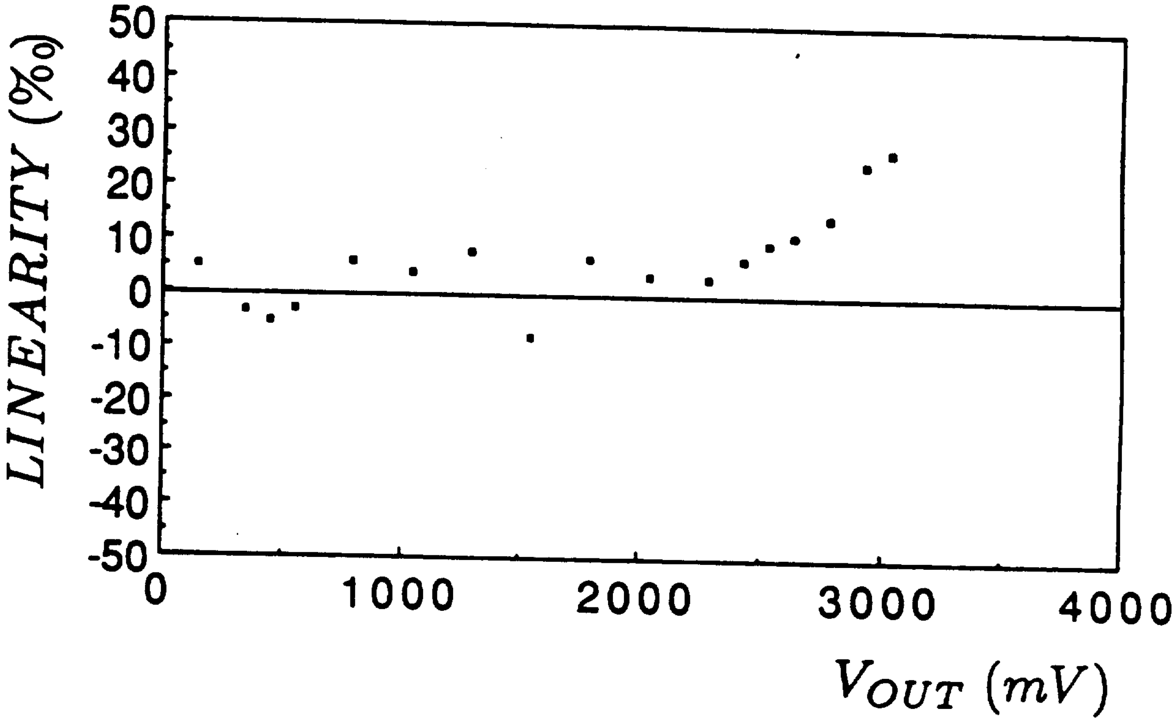

LINEARITY (%0)
50
40
30
20
10
0
-10
-20
-30
-40
-50
0
1000
2000
3000
4000
VOUT (mV)

Fig.10

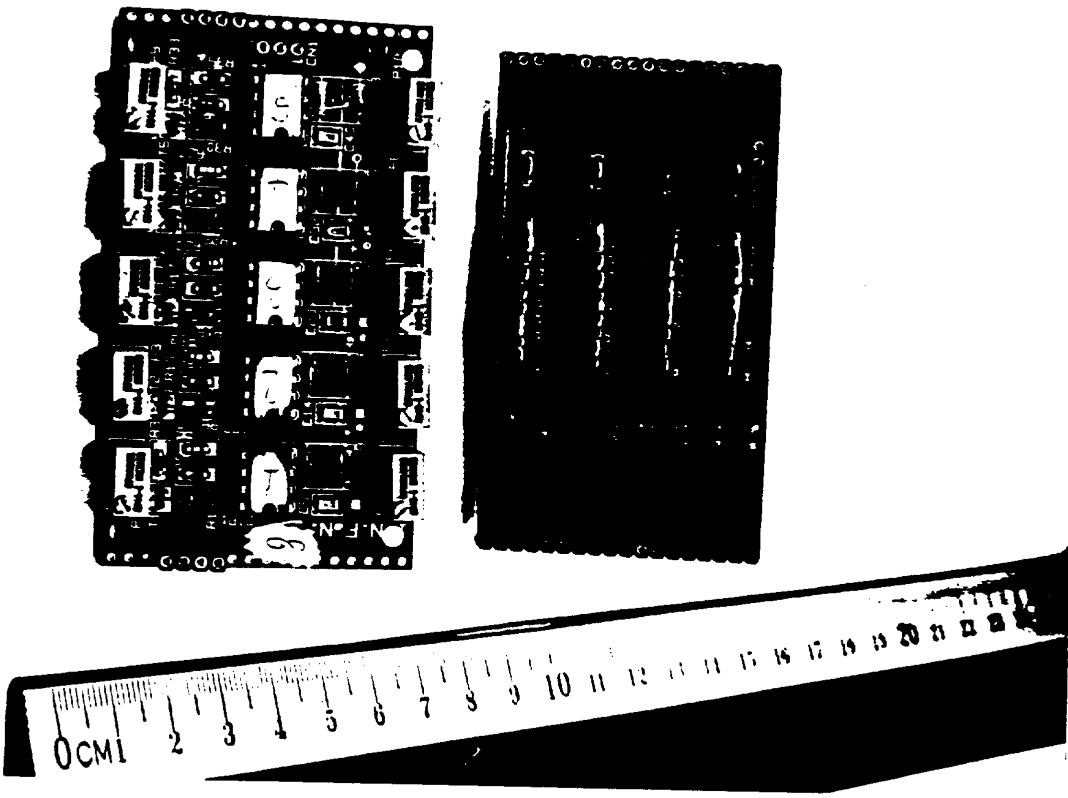

Fig.11

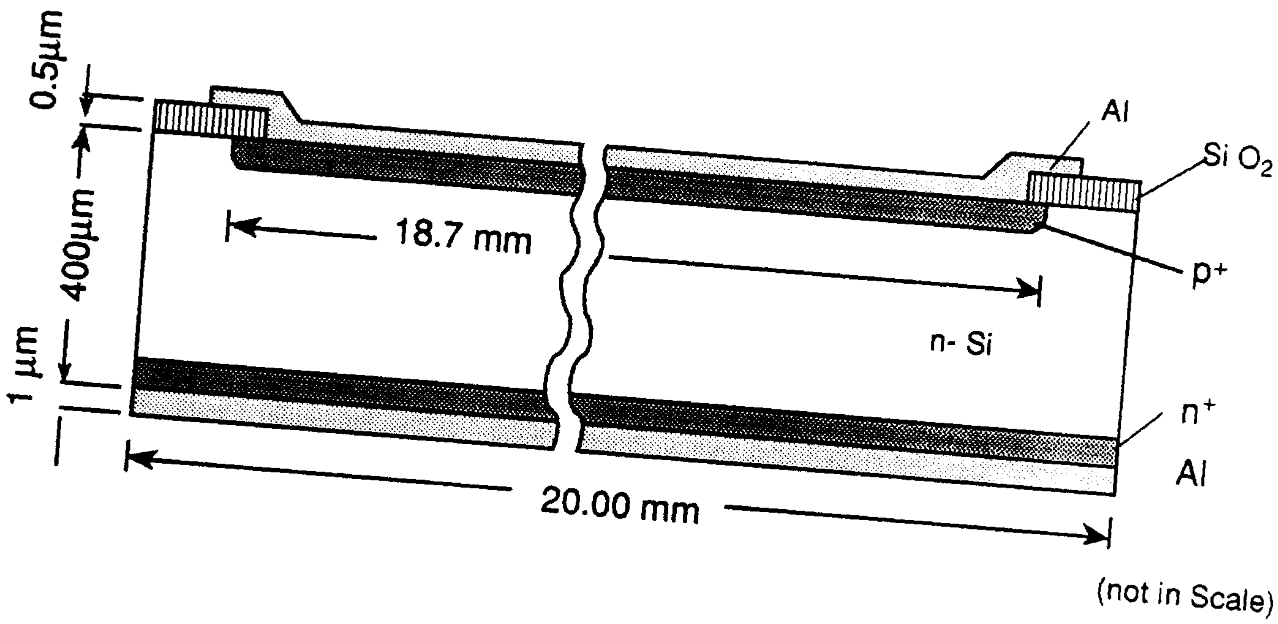

Fig. 12

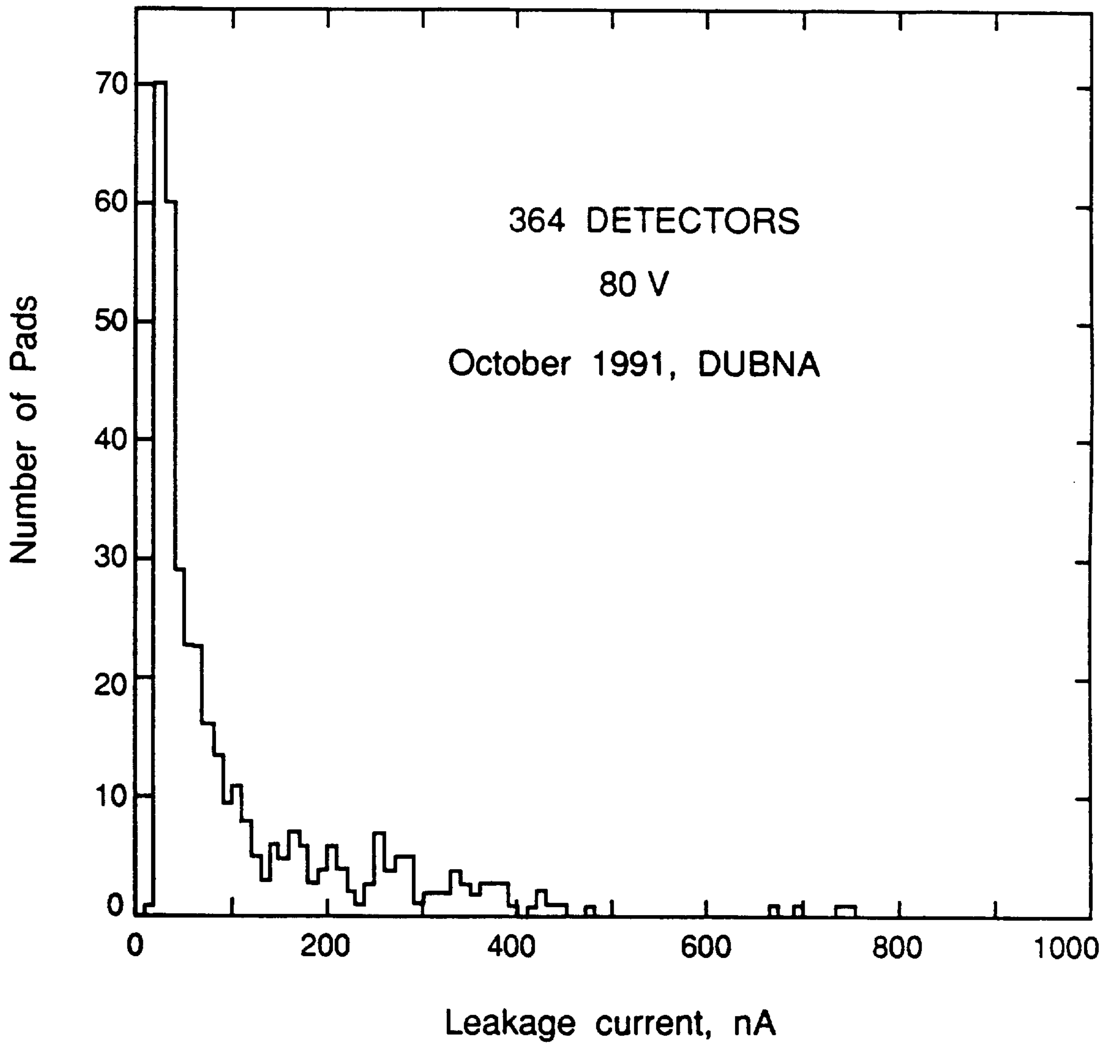

364 DETECTORS
80 V
October 1991, DUBNA
Number of Pads
0
10
20
30
40
50
60
70
0
200
400
600
800
1000
Leakage current, nA

Fig. 13

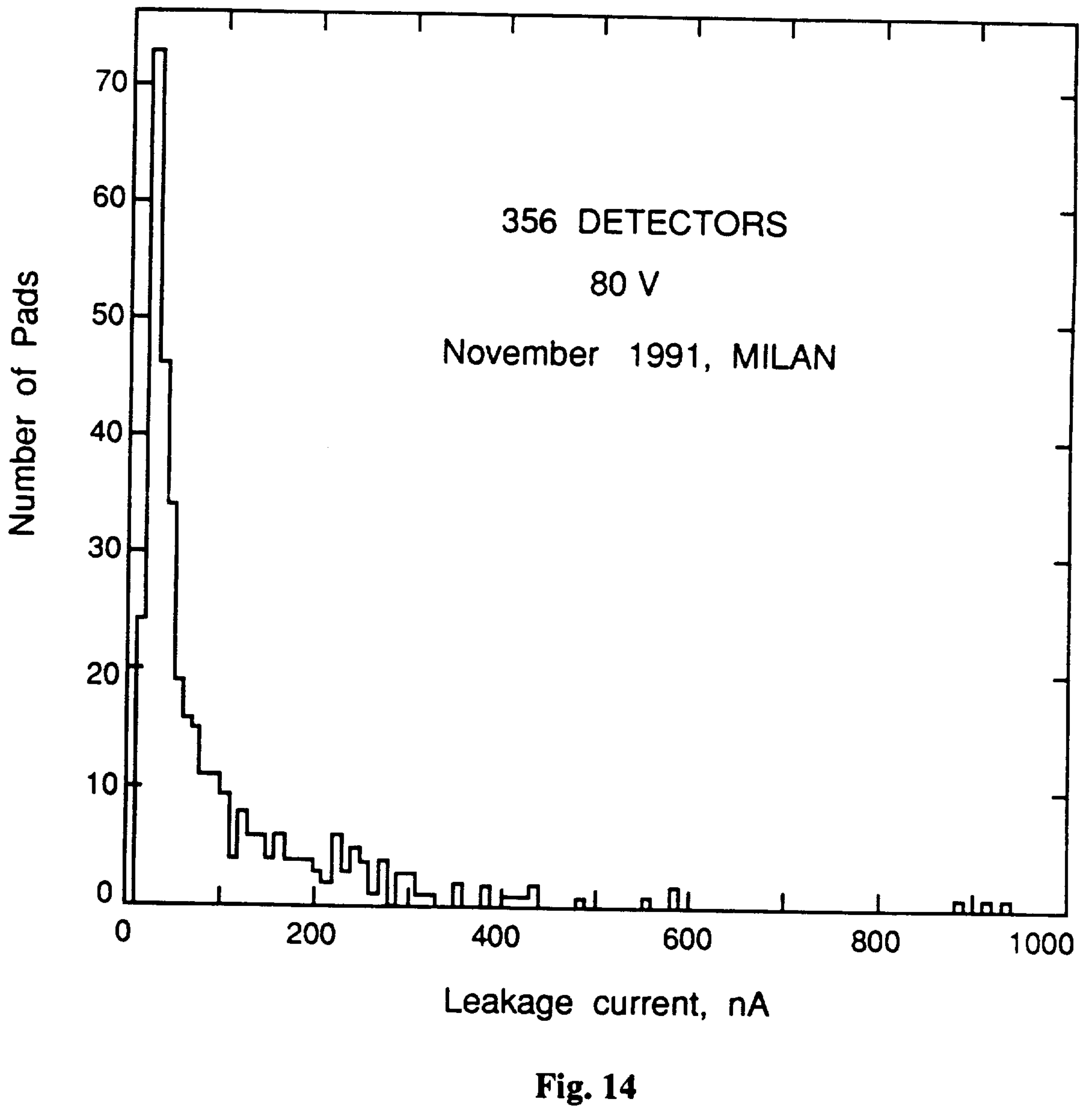

356 DETECTORS
80 V
November 1991, MILAN
Number of Pads
0
10
20
30
40
50
60
70
0
200
400
600
800
1000
Leakage current, nA

Fig. 14